PCCP

Accepted Manuscript

ROYAL SOCIETY OF CHEMISTRY

www.rsc.org/pccp

Dynamics of polymer adsorbed to an attractive homogeneous flat surface

Qing-Hui Yang[a], Chang-Ji Qian[b], Hong Li[b] and Meng-Bo Luo*[a]

The adsorption of a bond fluctuation self-avoiding walk polymer on an attractive homogeneous flat surface at temperature below critical adsorption point is studied using dynamic Monte Carlo simulation. Results show that the apparent size $R_{g,xy}^2$ of the polymer parallel to the surface increases exponentially with time during the adsorption process. The relaxation time for $R_{g,xy}^2$ reaching its asymptotic value σ_{eq} decreases with the increase in the polymer-surface attraction strength $E_{ps,}$ whereas σ_{eq} increases with E_{ps}, indicating that polymer is adsorbed faster and becomes more extended at stronger adsorption. The polymer's asphericity A_{xy} parallel to surface is sensitive to intra-polymer interaction and its behavior is different from that of $R_{g,xy}^2$. Simulation results also show that the two-dimensional behaviors of $R_{g,xy}^2$ and A_{xy} are different from that of the three-dimensional conformational size R_g^2 and asphericity A during the adsorption process. During the adsorption, the surface contacted monomer number M increases with time, but R_g^2 and A show novel behavior as they first increase with M at small M, then decrease with M at moderate M and finally increase with M again at large M. Whereas $R_{g,xy}^2$ and A_{xy} first decrease with M and then increase with M during the adsorption.

[a]*Department of Physics, Zhejiang University, Hangzhou 310027, China*
E-mail: luomengbo@zju.edu.cn
[b]*Department of Physics, Wenzhou University, Wenzhou 325035, China*

1 Introduction

The properties of polymers near surfaces or adsorbed on surfaces have received extensive interest and have been widely discussed[1]. A detailed understanding of the static and dynamic properties of polymer on surfaces is important for many chemical and biological processes[2-5], such as size-exclusion chromatography, polymer adhesion, colloidal stabilization, development of composite materials[6], coating and lubrication[7], DNA segregation in bacteria[8], and DNA packaging in viruses[9].

It is well known that a single chain adsorbed on attractive surfaces exhibits a phase transition from a desorbed state to an adsorbed state at critical adsorption point (CAP). In theoretical study of the adsorption of polymer, the polymer is often represented by a self-avoiding walk (SAW) on the simple cubic (sc) lattice and with one end grafted on the surface[10]. Every walk contacting the surface is assigned an attraction energy $-E$ (or a scaled energy $\varepsilon = E/k_BT$ with k_B the Boltzmann constant and T the temperature). The polymer chain can be adsorbed or desorbed depending on the scaled energy ε. Though the value of CAP is dependent on the polymer model[10-13], the adsorption transition can be always observed.

More monomers are adsorbed on surface with the decrease in the temperature or increase in the surface attraction. For SAW polymer in the absence of intra-polymer attraction, polymer conformation changes from three-dimensional (3D) extended coil to quasi-two-dimensional extended coil at CAP for infinitely long polymer or far below CAP for finitely long polymer[11]. Therefore, the statistical size of polymer parallel to surface is increased obviously below CAP whereas that perpendicular to surface is decreased significantly[10-13]. The adsorbed phase is named as Adsorbed-Extended (AE) phase as the polymer extends itself on the surface. Whereas for the SAW polymer with intra-polymer attraction, there is another adsorbed state named Adsorbed-Collapsed (AC) phase at which the polymer behaves as a dense liquid drop if the intra-polymer attraction is strong enough[14,15]. However, even for the AC phase, the statistical size of polymer parallel to surface is still increased after it is adsorbed on surface[16,17].

Besides the equilibrium properties of polymer, the dynamic properties of adsorbed polymer are also interesting. The diffusion of adsorbed polymer parallel to the surface was found to be a normal diffusion, but the exponent for the relaxation time is different from that of polymer in solution[11]. Shaffer has studied the adsorption time τ_{ads} of SAW polymer adsorbed to strong attractive surface using Monte Carlo (MC) simulation[18]. The scaling relation $\tau_{ads} \sim N^{1.58}$ was observed, where N is the polymer length. In this case, the adsorption would be very fast since the exponent 1.58 is smaller than that of relaxation time τ_R of polymer in good solvent. The same scaling was found for fast adsorption by Ponomarev *et al*. even if an activation barrier for polymer to desorb was introduced in their simulations[19]. For the fast adsorption, the adsorption follows a zipping mechanism whereby the chain adsorbs predominantly by means of sequential, consecutive attachment of monomers[19]. Based on the zipping mechanism, a scaling relation $\tau_{ads} \sim N^{1+\nu}$ was predicted and confirmed by MC simulations[20,21]. Here ν is the Flory exponent, which is about 0.6 for 3D SAW polymers.

However, the adsorption process was complex and was dependent on many factors, e.g. length and chemical nature of polymer[22]. Recently, the transient response of DNA molecules on a rigidly supported lipid membrane upon their adsorption was investigated by using real-time single-molecules imaging technique[23]. Two-dimensional (2D) apparent size $R_{g,xy}^2$ and asphericity A_{xy} were estimated through the fluorescent intensity of image of DNA. $R_{g,xy}^2$ is the surface parallel component of the square radius of gyration R_g^2. The attraction between DNA and surface was tuned by changing the molar fraction Φ_{DOTAP} of 1,2-dioleoyl-3-trimethylammonium-propane (DOTAP) in the adsorbent membrane. After landing fluorescent DNA molecules onto the adsorbent membrane, these DNA coils gradually relax and expand their 2D apparent sizes. Though the evolution of $R_{g,xy}^2$ exhibits considerable variations among individual molecules, the

ensemble-averaged size $< R^2_{g,xy} >$ can be characterized by a generic exponential relaxation. This evolution defines the primary relaxation timescale, which varies with the lipid composition of the membrane. The results indicated that the interaction between the absorbed molecules and the lipid elements plays an important role in the relaxation of chain towards the final equilibrium[23]. Fluorescent image also revealed that the DNA molecule changes from sphere-like conformation with small A_{xy} to high anisotropic one with big A_{xy} during the adsorption[23].

In the present work, we study the adsorption of a SAW polymer on an attractive flat surface using dynamic MC method in a sc system. We consider a homogeneous surface where each site of the surface produces identical attraction to polymer. In this case, a polymer monomer will gain energy if it locates at the nearest neighbor site of the surface. Simulations are carried out at temperature below CAP of polymer. We have studied the evolution of polymer's conformational properties at the beginning of the adsorption process. The response of polymer's apparent size is consistent with the experiment of DNA adsorption[23]. With the increase in the attraction strength, the equilibrium apparent size increases but the relaxation time for the polymer reaching equilibrium decreases. However, we find that the response of polymer's shape is more complicated. On the other hand, the detailed variation of polymer's conformational properties on the polymer-surface contact number M is also investigated. Results show that both 3D size and asphericity present a maximum at small M and minimum at moderate M, whereas the 2D apparent size and apparent asphericity decrease with M at first and then increase with M.

2 Simulation model and method

The simulation system is a cuboid with the length L_x, L_y, and L_z in the x, y, and z directions, respectively. Periodic boundary conditions (PBC) are adopted in the x and y directions parallel to the surface. An infinitely large flat surface is placed at $z = 0$. The surface is impenetrable for polymer but produces homogeneous attraction to polymer, i.e., it attracts polymer to the nearest neighbor (NN) layer at $z = 1$ with NN

polymer-surface attraction $-E_{ps}$. Here, polymer's monomer at $z = 1$ gives a surface contact.

We consider a 3D coarse-grained bond-fluctuation SAW polymer model on the sc lattice. The polymer chain of length N is composed of N sequential linked monomers numbered from 1 to N. Each monomer occupies one lattice site and the bond length between two sequential monomers is allowed to vary among 1, $\sqrt{2}$, and $\sqrt{3}$ [18,24]. However, bond crossing is not allowed in this model. Here, monomers do not correspond to specific atoms in a polymer but rather to small groups of atoms, and the bonds do not represent specific covalent bonds between two atoms but instead the linkages between monomers. Besides the SAW of polymer monomers, we take into account the intra-polymer NN monomer-monomer attraction $-E_{pp}$. The statistical dimension of polymer chain decreases with the increase in E_{pp}.

The dynamics of the polymer is achieved through bond fluctuation and Metropolis algorithm[25,26]. For each trial move, we randomly choose a monomer and let it move to one of its six NN sites. The new site is picked up randomly, too. We then check the new site to find out whether it satisfies simultaneously the following three requests: (1) empty, (2) without violating bond crossing, and (3) bond length being allowed. If the new site satisfies the three requests, the trial move will be accepted with a probability $p = \min[1, \exp(-\Delta E/k_B T)]$, where ΔE is the energy shift due to the move, otherwise we give up this trial move. Such kind single monomer move will continue until the preset condition is satisfied. The time unit is one Monte Carlo step (MCS), during which N trial moves are tried. That is, every monomer is tried to move one step in average during one MC.

In the simulation, we have placed an additional repulsive surface at $z = L_z$ in order to prevent the polymer diffusing away from the attractive surface. The repulsive surface mimics the solution-air interface in the experiment, which restricts the polymer locate in between two surfaces. However, L_z is much large than the dimension of polymer R_{g0}, the radius of gyration in bulk solution, so that the effect of the upper surface on the adsorption of polymer on the lower surface can be

neglected[27]. At the beginning of every simulation run, a polymer is generated and equilibrated without contacting with the attractive surface. To this end, we introduce a virtual repulsive surface at z = L_z/4, and generate and equilibrate the polymer always above the virtual surface. After a sufficient long random moves of the polymer, set as about $N^{2.2}$ (~ $N^{1+2\nu}$) MCS, the polymer is assumed to have reached the equilibrium state between the upper and the virtual surfaces. We then set the time as t = 0 at this moment, remove the virtual surface, and let the polymer random diffuse for another long time t_{stat} which is used for statistics. At time t_0, which is shorter than t_{stat}, the polymer begins to contact with the lower attractive surface and the adsorption of polymer starts. The conformational properties are recorded during the period form t = 0 to t_{stat}.

We intend to study the transient response of a SAW polymer model on an attractive homogeneous flat surface. The CAP of the SAW polymer model at E_{pp} = 0 was estimated to be k_BT_c = 1.625 for E_{ps} = 1[13], that is, at $\varepsilon_c = E_{ps}/k_BT_c$ = 0.615. In this work all simulations are carried out at temperature k_BT = 1 below the CAP of the SAW polymer. The simulation size is chosen as $L_x = L_y = N$, so that there is no size effect on the polymer in the x and y directions. While $L_z > 5R_{g0}$ is used so that the size effect in the z direction is negligible[27]. We have counted the time dependence of the polymer conformation, including size and shape, and surface contact number. Simulation results are averaged over 5000 independent runs and the statistical error is small.

3 Results and discussion

During the simulation, we have monitored the variation of the surface contact number M, square radius of gyration R_g^2 and its component parallel to surface $R_{g,xy}^2$. Figure 1 shows the variation of $R_{g,xy}^2$ and M of a typical simulation run for polymer length N = 100 and interactions E_{pp} = 0.1 and E_{ps} = 1. One can see a sudden adsorption accompanying a step increase in M at $t_0 \approx 0.24\times10^6$. In fact, such a sudden adsorption is observed in every simulation run though t_0 varies with simulation sample, which is

in agreement with the experimental observation[23]. We find that both $R^2_{g,xy}$ and M fluctuate strongly with time even if the polymer reaches a fully adsorbed state with a large value of M. Though the large fluctuation of $R^2_{g,xy}$ and M, the polymer is always adsorbed on the surface since simulations are performed below the CAP of polymer.

The inset of Fig. 1 shows the duration time $t(M)$ for the polymer spending at every specific contact number $M > 0$. One can see that the transient adsorption takes place from $M = 0$ to $M = 30$ and the duration for the adsorption is very short. After the transient adsorption, polymer diffuses randomly on the attractive surface with a large fluctuation in M. The peak value of M in the inset of Fig. 1 roughly corresponds to the averaged adsorbed monomers, which is dependent on the simulation parameters such as N, E_{pp}, and E_{ps} but is independent of t_{stat}.

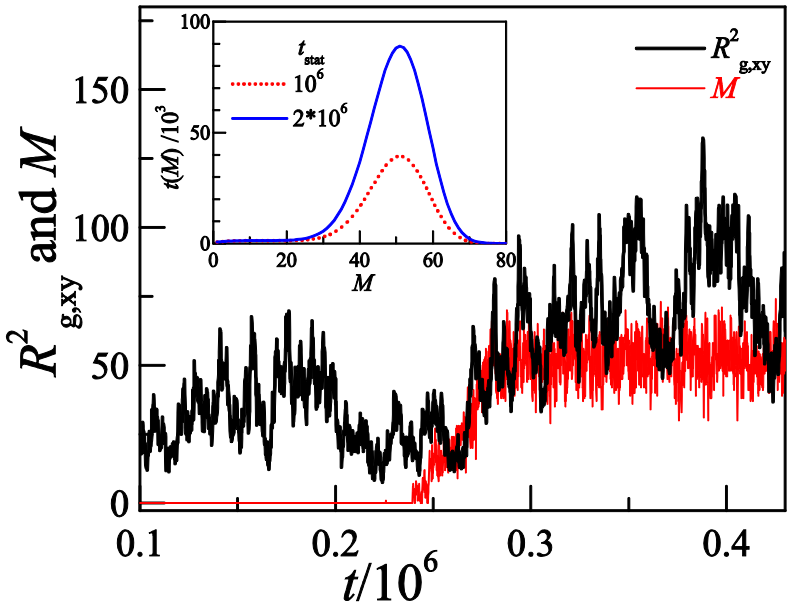

Fig. 1 Variation of the surface contact number M and the parallel component of square radius of gyration $R^2_{g,xy}$ for polymer adsorption. Polymer length $N = 100$, and interactions $E_{pp} = 0.1$ and $E_{ps} = 1$. The inset presents the duration time of polymer at different contact number $M > 0$.

We have calculated the mean-square radius of gyration $< R_{g,xy}^2 >$ as functions of the elapsed time $t–t_0$ for different polymer-surface attractions E_{ps}. Here <> represents an ensemble average over samples. Figure 2 shows the results for the polymer of length N = 100 and intra-polymer attraction strength E_{pp} = 0.1. We find from the inset (b) of Fig. 2 that $< R_{g,xy}^2 >$ increases smoothly with $t–t_0$ and saturates at long time. Here we can define the initial landing size of polymer as σ_{eq} at $t = t_0$ and the equilibrium size as σ_{eq} at large t. Using the analysis method introduced in experiment[23], we recast all data using the dimensionless variable $S \equiv \frac{< R_{g,xy}^2 > -\sigma_0}{\sigma_{eq} - \sigma_0}$, and dimensionless time $t^* \equiv \frac{t - t_0}{\tau}$ in the main panel of Fig. 2. Here τ is named as the relaxation time of polymer, which is a fitting parameter to obtain the best overlap of our simulation data. And we find that the simulation data can be roughly expressed by an exponential function $S = 1 - \exp(-t^*)$, similar to that of experiment[23]. The inset (a) of Fig. 2 also shows the variation of the relaxation time τ on the polymer-surface attraction strength E_{ps}. We find that τ decreases with E_{ps}, that is, the polymer can reach equilibrium more quickly at stronger surface attraction. We find that the equilibrium size σ_{eq}, equal to the saturated value shown in the inset (b) of Fig. 2, increases with E_{ps}. The reason is that polymer becomes more like a 2D conformation with the increase in E_{ps}. This is in agreement with other simulation results[10-13,17]. Such a behavior was also observed for the adsorption of polymer on spherical surface[28].

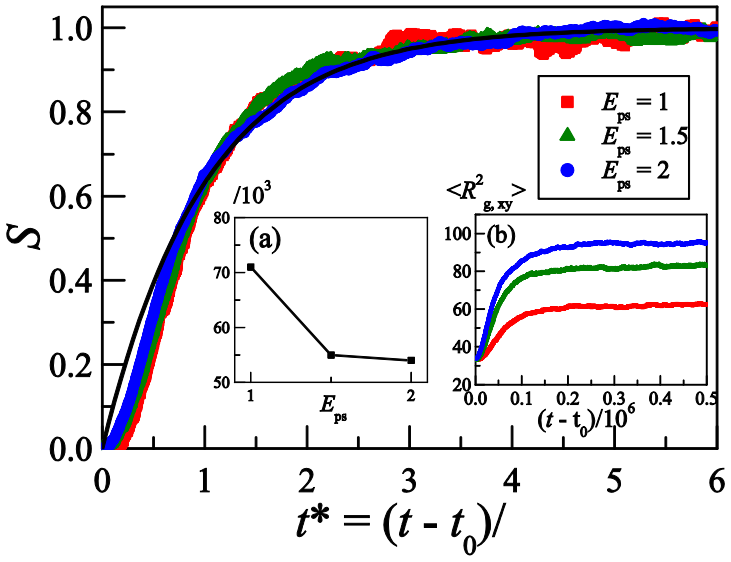

Fig. 2 Dependence of the dimensionless chain dimension S on the scaled time t^* for chain length N = 100 at different polymer-surface attractions E_{ps} = 1, 1.5, and 2. The solid black line gives the exponential function $S = 1 - \exp(-t^*)$. The inset (a) presents the relaxation time τ at different E_{ps}. The inset (b) presents the variation of $< R^2_{g,xy} >$ with the simulation time $t-t_0$. Here E_{pp} = 0.1 is used.

Figure 3a presents the dependence of the mean contact number <M> on the time $t-t_0$ for chain length N = 100 at different polymer-surface attractions E_{ps} = 1, 1.5, and 2. It is obvious that <M> tends to its saturated value quickly, which means that the chain is strongly adsorbed on the attractive surface. The time scale for the saturation is in the same order as the relaxation time τ. The time for saturation of <M> is also defined as the adsorption time τ_{ads} for polymer adsorption[21]. The behavior of τ is in agreement with τ_{ads}. It was found that τ_{ads} decreases with the increase in the surface attraction[21].

During the polymer adsorption, both $< R^2_{g,xy} >$ and <M> increase with time. The adsorption of polymer includes two processes: adsorption of polymer monomers to surface and extension of polymer conformation on surface. The former will increase the surface contact number M while the latter will increase the apparent size $R^2_{g,xy}$. Our results show that these two processes take place simultaneously. The time

scale τ for the evolution of $< R^2_{g,xy} >$ and <*M*> however decreases with the increase in the surface attraction E_{ps}, that is, the adsorption of polymer becomes faster on a stronger attractive surface.

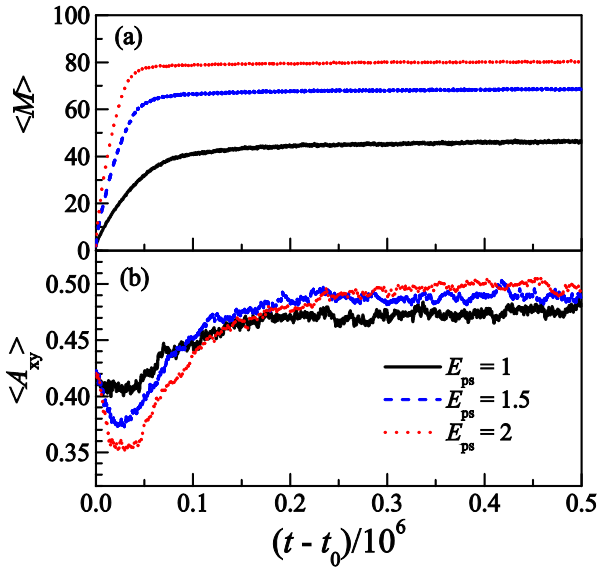

Fig. 3 Dependence of the mean contact number <*M*> (a) and the mean asphericity <A_{xy}> (b) on the simulation time $t–t_0$ for chain length N = 100 at different polymer-surface attractions E_{ps} = 1, 1.5, and 2. Here E_{pp} = 0.1 is used.

The dependence of the mean asphericity <A_{xy}> on the simulation time $t–t_0$ is presented in Fig. 3b. <A_{xy}> represents the 2D shape of polymer chain parallel to the surface, which is defined as $A_{xy} = \frac{(L_1^2 - L_2^2)^2}{(L_1^2 + L_2^2)^2}$, in which L_1^2 and L_2^2 are two eigenvalues of a 2D gyration tensor[29]

$$S_{xy} = \frac{1}{N}\sum_{i=1}^{N} s_i s_i^{\mathrm{T}} = \begin{pmatrix} S_{xx} & S_{xy} \\ S_{xy} & S_{yy} \end{pmatrix}, \quad (1)$$

where $s_i = \mathrm{col}(x_i, y_i)$ is the position vector of monomer *i* in a frame of reference with its origin at the center of mass of whole polymer chain, and s_i^{T} is the transposed matrix of s_i. The tensor S_{xy} can be diagonalized with two eigenvalues L_1^2 and L_2^2.

The trace of the tensor S_{xy} is equal to $R_{g,xy}^2$ with $R_{g,xy}^2 = L_1^2 + L_2^2$.

The variation of the 2D asphericity $<A_{xy}>$ with time is different from that of the apparent size $< R_{g,xy}^2 >$ and shows somewhat more complex. $<A_{xy}>$ first decreases quickly to a minimum and then increases slowly with time and at last saturates. And we find that $<A_{xy}>$ varies more obviously at large E_{ps}. We find that both the minimum value and the saturated value are dependent on the polymer-surface attraction strength E_{ps}. The minimum value decreases with the increase in E_{ps}, whereas the saturated value increases with E_{ps}. For the strong adsorbed case with $E_{ps} = 2$, the saturated value of $<A_{xy}>$ is about 0.5, which is close to the simulation results for 2D polymer, e.g. 0.506 for polymer length $N = 201$[30] and 0.503 for $N = 101$[31]. This indicates that the conformation of adsorbed polymer is roughly 2D.

It is well known that the conformations of polymer are dependent on the intra-polymer attraction E_{pp}. There are rich phases for polymer adsorption when the intra-polymer attraction is taken into account[14-16]. For polymer near a weak attractive surface, a Desorbed-Extended (DE) phase will change to a Desorbed-Collapsed (DC) phase with the increase in E_{pp}. Whereas for polymer near a strong attractive surface, the AE phase changes to AC phase with the increase in E_{pp}. Because of the competition between intra-polymer attraction and polymer-surface attraction, the equilibrium conformations of adsorbed polymer are complicated but has been extensively studied[14-17,32,33]. In this work, we investigate the influence of intra-polymer attraction E_{pp} on the adsorption dynamics of polymer. Specifically, we study the transient adsorption process of polymers with weak intra-polymer attraction $E_{pp} = 0.1$, critical attraction $E_{pp}^* = 0.5$, and strong one $E_{pp} = 1$.

The equilibrium conformations of polymer chain at t_0 are dependent on E_{pp}. At weak attraction $E_{pp} = 0.1$, the polymer is a random extended coil with a large statistical size $< R_{g,xy}^2 > \approx 33$ and an asphericity $<A_{xy}> \approx 0.42$. The size of polymer becomes relatively small with the increase in E_{pp}, for instant, we have $< R_{g,xy}^2 > \approx 7.2$ and $<A_{xy}> \approx 0.18$ at $E_{pp} = 0.5$ and $< R_{g,xy}^2 > \approx 4.1$ and $<A_{xy}> \approx 0.077$ at $E_{pp} = 1$.

Actually, the polymer is roughly a compact sphere at E_{pp} = 1. The coil-to-globule transition or DE-DC boundary is estimated to take place at E_{pp}^* = 0.5. Here, the critical value E_{pp}^* separates a weak intra-polymer attraction region with $E_{pp} < E_{pp}^*$ and a strong intra-polymer attraction region with $E_{pp} > E_{pp}^*$.

The final equilibrium adsorbed conformations of polymers are also dependent on E_{pp}[14,16]. The size $< R_{g,xy}^2 >$ at large t decreases obviously with the increase in E_{pp}, like the behavior of $< R_{g,xy}^2 >$ at t_0. It decreases from about 65 at E_{pp} = 0.1 to about 6.0 at E_{pp} = 1 for the case E_{ps} = 1, consistent with the simulation results on a hydrophobic-polar (HP) lattice protein model interacting with attractive surfaces[17]. However, the decrease in <M> with the increase in E_{pp} is less remarkable than $< R_{g,xy}^2 >$. We have <M> = 46 at E_{pp} = 0.1 and <M> = 32 at E_{pp} = 1 for the case E_{ps} = 1, indicating that the adsorption is still strong even for E_{pp} = 1. Generally speaking, the decreases of $< R_{g,xy}^2 >$ and <M> with the increase in E_{pp} are consistent with the phase diagram of polymer adsorption[14-16], where the state AE at weak intra-polymer attraction will change to the state AC at strong intra-polymer attraction.

But the time-dependent behavior of the dimensionless chain dimension S is roughly independent of E_{pp}. Though the value of $< R_{g,xy}^2 >$ decreases with the increase in E_{pp}, the behavior of S at $E_{pp} = E_{pp}^*$ and $E_{pp} > E_{pp}^*$ is roughly the same as that presented for E_{pp} = 0.1. Therefore, one could conclude that the dynamic behavior of apparent size $< R_{g,xy}^2 >$ is independent of intra-polymer attraction.

However, the dependence of the 2D asphericity <A_{xy}> on the time is strongly dependent on E_{pp}. Figure 4 presents <A_{xy}> for different E_{pp}s. Here we use E_{ps} = 2 as the variation of <A_{xy}> is more obvious at large polymer-surface attraction value as shown in Fig. 3b. The results for polymers with E_{pp} = 0.5 and E_{pp} = 1 are obviously different from that for polymer with weak attraction E_{pp} =0.1. The intra-polymer attraction assembles monomers together and makes both size and shape asphericity small. We find that <A_{xy}> also decreases with the increase in E_{pp} during the whole adsorption process. The initial value of <A_{xy}> at $t = t_0$ and the saturated value of <A_{xy}>

decrease with the increase in E_{pp}. Moreover, the decrement at the very beginning disappears for E_{pp} = 0.5 and 1. $<A_{xy}>$ however increases gradually with the adsorption time. Our results show that the shape of the adsorbed polymer is highly dependent on the intra-polymer attraction. The general tendency that $<A_{xy}>$ increases with time is in agreement with the experimental observation[23].

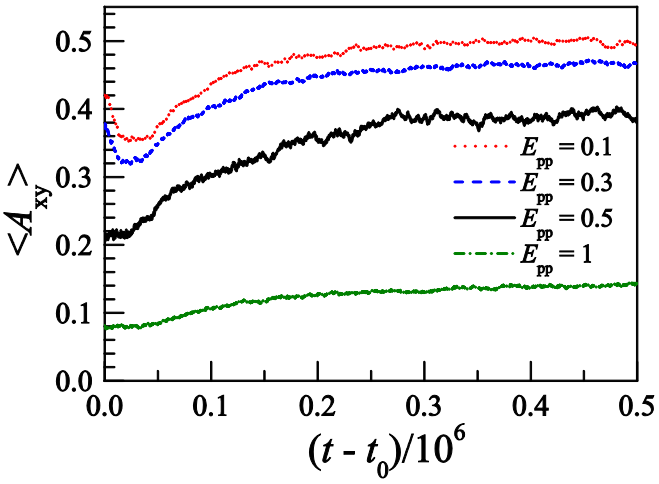

Fig. 4 Dependence of the mean asphericity $<A_{xy}>$ on the simulation time $t-t_0$ for chain length N = 100 with different intra-polymer attractions E_{pp} = 0.1, 0.3, 0.5, and 1. The polymer-surface attraction is E_{ps} = 2.

To better understand the adsorption of polymer chain, we have investigated how the properties of polymer change with the adsorbed monomer number or the surface contact number M. Specifically, we have calculated the size and shape of polymer at different M during the adsorption process. As both the size and M change with time as shown in Fig. 1, we then calculate the averaged values of square radius of gyration R_g^2 and surface parallel component $R_{g,xy}^2$ over M in one independent sample. The number for averaging in one sample is equal to the duration time $t(M)$ shown in the inset of Fig. 1. And it is often very large, for example, we have $t(M = 1) \approx 600$. Such a phenomenon is due to the random nature of the adsorption, i.e., adsorption/desorption of monomers takes place randomly in the simulation. Therefore, both R_g^2 and $R_{g,xy}^2$ are averaged over a large number of conformations even in one single simulation run.

Finally, we obtain mean-square radius of gyration $< R_g^2 >$ and its parallel component $< R_{g,xy}^2 >$ by averaging them over 5000 independent samples again. Figure 5 presents the variation of $< R_g^2 >$ and $< R_{g,xy}^2 >$ with M for polymer with chain length N = 100 at E_{pp} = 0.1 and E_{ps} = 1. The values at M = 0 correspond to the situation that the polymer is in the solution without contacting with the attraction surface.

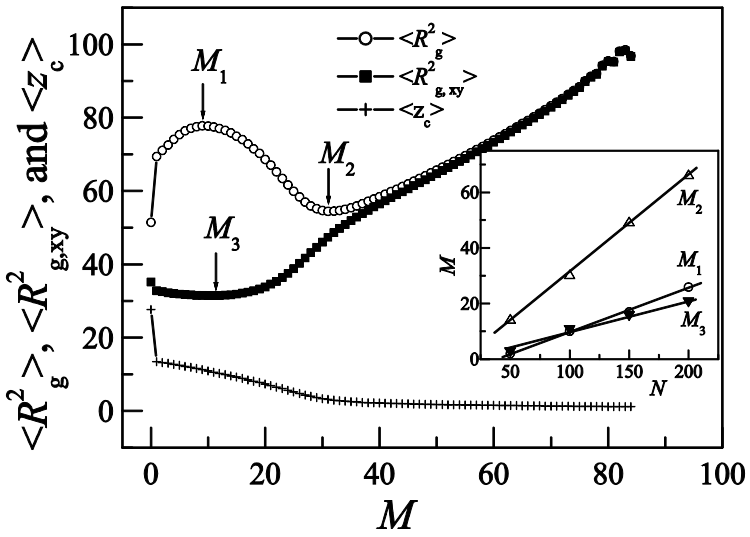

Fig. 5 Plots of the sizes $< R_g^2 >$, $< R_{g,xy}^2 >$, and center of mass <z_c> versus the surface contact number M for chain length N = 100 with intra-polymer attraction E_{pp} = 0.1. The polymer-surface attraction is E_{ps} = 1. M_1 and M_2 correspond to the peak and valley of the $< R_g^2 >$ curve, respectively. M_3 corresponds to the valley of the $< R_{g,xy}^2 >$ curve. The inset shows the polymer length dependence of values M_1, M_2, and M_3.

It is interesting to see that $< R_g^2 >$ increases fast from M = 0 to M = 1. When the polymer begins to be adsorbed, the monomers near the surface move downwards due to the surface's attraction whereas other monomers still locate at their original sites. This will obviously increase the size of polymer by lowering the center of mass. However, such z-direction motion does not affect the transverse size parallel to

surface, thus the value $< R_{g,xy}^2 >$ only shows a small decrease. The phenomenon is similar to the stem-flower picture with simple zipping mechanism for fast polymer adsorption[19-21].

We have measured the end-to-end vector auto-correlation function $\rho(t)$ of the polymer chain, which is defined as[34]

$$\rho(t) = \frac{< \vec{R}(t) \cdot \vec{R}(0) >}{< R^2 >}. \quad (2)$$

Here $\vec{R}(t)$ and $\vec{R}(0)$ are the end-to-end vectors at time *t* and at time 0, respectively. $\rho(t)$ decays exponentially with time, i.e., $\rho(t) \sim \exp(-t/\tau_R)$. From our simulation, τ_R is estimated to be about 33000 for the polymer with N = 100 and E_{pp} = 0.1 in bulk solution. Whereas the total time for polymer changing from M = 1 to the place of the first peak M_1 = 10 shown in Fig. 5 is about 10000. Therefore, the relaxation time of the end-to-end vector is much larger than the adsorption time of the first few monomers from M = 1 to M = 10. Thus the polymer does not have enough time to adjust its conformation during the beginning of adsorption. This results in the increase of $< R_g^2 >$ at small M shown in Fig. 5. For fast adsorption, the stem-flower scenario actually presented such a behavior[20,21]. The predicted adsorption time $\tau_{ads} \sim N^{1+\nu}$ of long polymers adsorbed to strong attractive surfaces is shorter than the relaxation time $\tau_R \sim N^{1+2\nu}$ of polymers in dilute solution[19-21]. It is important to note that this phenomenon is due to the dynamical process of the transient adsorption. That is, the system is out-of-equilibrium during the transient adsorption process. And we conclude that M_1 results from the competition between relaxation of polymer and adsorption rate of polymer.

The mean-square radius of gyration $< R_g^2 >$ decreases with the further increase in M because more and more monomers are adjacent to the surface. Therefore the component normal to the surface decreases gradually. $< R_g^2 >$ reaches its minimum at place M_2. The elapsed time from M = 1 to M_2 = 30 is about 40000, slightly larger

than the relaxation time τ_R. Therefore the phenomenon of minimum of $< R_g^2 >$ seems to be somewhat close to an equilibrium property. Similar phenomenon was observed in annealing simulation of an end-grafted polymer on an attractive surface, as there is a minimum of $< R_g^2 >$ near CAP[35]. In the annealing simulation, the surface contact number increases with the decrease in the simulation temperature. At $M > M_2$, $< R_g^2 >$ increases gradually with M. The increase of $< R_g^2 >$ beyond M_2 is due to the roughly fully adsorption of polymer. The polymer chain behaves like a 2D structure on the surface[35].

The adsorption can also be described from the variation of polymer center away from the attractive surface. The mass center of the polymer $<z_c>$ is calculated and is plotted against the surface contact number M in Fig. 5. We find that $<z_c>$ decreases with M and is close to 1 at M_2. It is clear to see that the polymer chain tends to be fully adsorbed on the surface at M_2.

As shown in Fig. 5, the mean apparent size $< R_{g,xy}^2 >$ parallel to surface however shows different behavior from $< R_g^2 >$. It decreases slightly with M at small M and then increases gradually with M. There is a minimum of $< R_{g,xy}^2 >$ located at M_3 which is close to M_1. Because the decrease is not significant, it is not observed in the time dependence behavior shown in Fig. 2 where $< R_{g,xy}^2 >$ is averaged over time. The reason is that M can be different at the same adsorption time for different simulation samples. After M_3, the polymer chain begins to extend itself along the surface with more monomers being adsorbed, and therefore the size $< R_{g,xy}^2 >$ increases continuously with M. The result indicates that polymer becomes more extended at stronger adsorption. This is also consistent with the result that the adsorbed size σ_{eq} increases with E_{ps}. At M_2, one finds $< R_{g,xy}^2 > \approx < R_g^2 >$, which means that the normal component tends to 0 and the polymer tends to fully contact with the surface.

The inset of Fig. 5 shows that all M_1, M_2, and M_3 increase linearly with polymer

length N for E_{pp} = 0.1. The same relationship is observed for strong intra-polymer attraction E_{pp} = 1. In fact, such linear relations are observed at different E_{pp}s, but the slopes are dependent on E_{pp}.

Values of M_1, M_2, and M_3 are also dependent on the interactions E_{pp} and E_{ps}. The dependence of M_1, M_2, and M_3 on E_{ps} is relatively simple and is roughly independent of E_{pp}. We find that M_1 and M_2 increase with the increase in E_{ps} whereas M_3 is roughly a constant. However, the dependence of M_1, M_2, and M_3 on E_{pp} is slightly complicated. Figure 6a plots M_1, M_2, and M_3 at different E_{pp}s. We find that M_1 and M_2 show the similar behavior. They at first increase with E_{pp} at about $E_{pp} < E_{pp}^*$, then decrease with E_{pp} after E_{pp}^*, and at last they saturate after E_{pp} = 0.75. Whereas M_3 shows different behavior: it decreases with E_{pp} at small E_{pp}, reaches 0 near E_{pp}^*, and again reaches none zero value at large E_{pp}. It is interesting to see that M_3 is about 0 near E_{pp}^*. The case M_3 = 0 indicates that $< R_{g,xy}^2 >$ monotonically increases with M during the adsorption. It is also interesting to see that $M_3 > 0$ at large E_{pp}, indicating that $< R_{g,xy}^2 >$ decreases at the beginning of the adsorption even at $E_{pp} > E_{pp}^*$ where the polymer is quit compacted.

The dependence of $< R_g^2 >$s at M_1 and M_2 and $< R_{g,xy}^2 >$ at M_3 on E_{pp} is plotted in Fig. 6b. We find that all these values decrease obviously with E_{pp} at $E_{pp} < E_{pp}^*$, and tend to be constants at $E_{pp} > E_{pp}^*$. Because $< R_{g,xy}^2 >$ is small at $E_{pp} > E_{pp}^*$, the absolute decrease in $< R_{g,xy}^2 >$ from M = 0 to $M = M_3$ is negligible at $E_{pp} > E_{pp}^*$. However, the relative decrease is still visible, e.g. about 10% at E_{pp} =0.1 and about 8% at E_{pp} = 0.7.

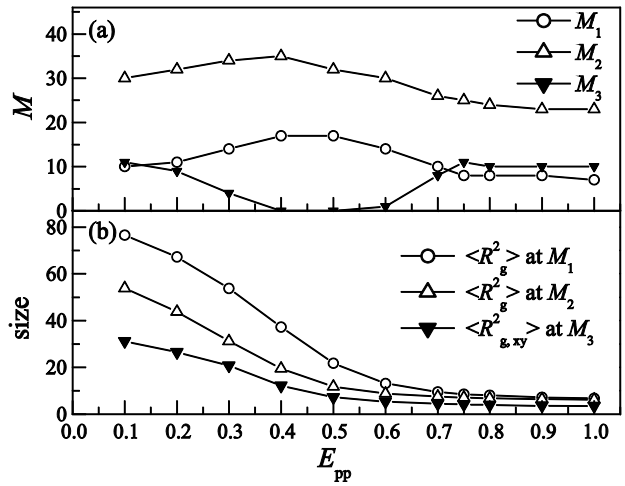

Fig. 6 Plots of M_1, M_2, and M_3 (a) and $< R_g^2 >$ at M_1 and M_2 and $< R_{g,xy}^2 >$ at M_3 (b) versus the intra-polymer attraction E_{pp} for polymer length N = 100 and polymer-surface attraction E_{ps} = 1.

During the adsorption, M increases with time as shown in Fig. 3a. Therefore we could expect that the peak M_1 and the valley M_2 can be observed in the time dependent behavior of $< R_g^2 >$. Figure 7 plots the time dependent behavior of $< R_g^2 >$ for polymer with N = 100 at E_{pp} = 0.1. At E_{ps} = 1.5 and 2, one could see that $< R_g^2 >$ first increases and then decreases at the very beginning, like the behavior of $< R_g^2 >$ shown in Fig. 5. Such a behavior is obviously different from the time dependent behavior of $< R_{g,xy}^2 >$ shown in Fig. 2. Therefore the behaviors observed in experiment for the apparent properties might be different from that of 3D properties. The disappearance of the peak for E_{ps} = 1 might be due to its relatively weak attraction. The adsorption takes longer time for a weaker attraction, therefore the peak might be averaged out because of dynamical process of the adsorption.

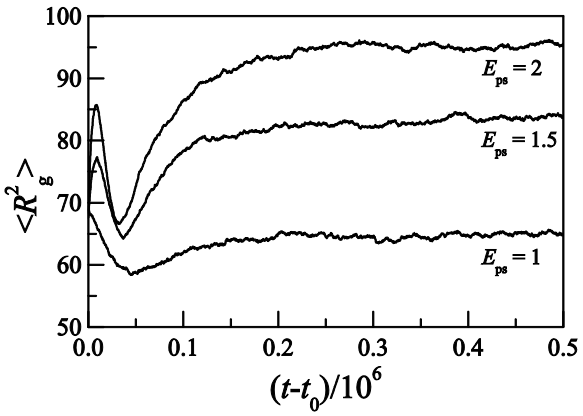

Fig. 7 Dependence of mean-square radius of gyration $< R_g^2 >$ on the simulation time $t-t_0$ for chain length N = 100 with different polymer-surface attractions E_{ps} = 1, 1.5, and 2. The intra-polymer attraction is E_{pp} = 0.1.

We have also studied the response of the asphericity of polymer chain to the contact number during the adsorption of polymer. The mean values of 3D asphericity <A> and that of 2D asphericity <A_{xy}> are calculated. Analogous to A_{xy}, A is calculated from a 3D gyration tensor[29]. Figure 8 presents the variation of <A> and <A_{xy}> on M for polymer length N = 100 at E_{pp} = 0.1 and E_{ps} = 1. The behavior of <A> is similar to that of $< R_g^2 >$ while that of <A_{xy}> is similar to that of $< R_{g,xy}^2 >$ (Fig. 5), which is in agreement with the positive correlation between shape and size for a linear polymer[36]. The increase in <A> at small M is corresponding to the elongation of polymer at the beginning of adsorption, while the decrease in <A> at moderate M is corresponding to the contraction of polymer as polymer moving down to surface, and the finial increase in <A> to the extension of polymer on surface. But our results show that the changes of shape and size are not in phase. The peak of <A> is at M_1, but the valleys of <A> and <A_{xy}> are not at M_2 and M_3, respectively. However, they are close to M_2 and M_3 due to the positive correlation between shape and size.

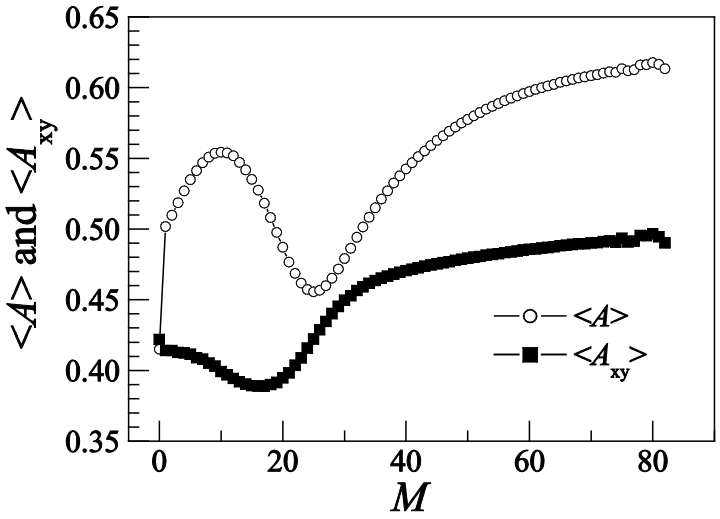

Fig. 8 Plots of the 3D asphericity $\langle A \rangle$ and 2D asphericity $\langle A_{xy} \rangle$ versus the surface contact number M for polymer length $N = 100$ with intra-polymer attraction $E_{pp} = 0.1$ and polymer-surface attraction $E_{ps} = 1$.

At $M = 0$, the values $\langle A \rangle \approx 0.41$ and $\langle A_{xy} \rangle \approx 0.42$ are consistent with the fact that the instantaneous shape of a polymer is not spherical in 3D view as well as in 2D view. Here $\langle A \rangle \approx 0.41$ for the polymer before adsorption is close to the simulation result 0.431 for polymer in dilute solution[30]. Though $\langle A_{xy} \rangle$ decreases with M at the beginning of the adsorption, it increases at moderate M and roughly saturates at large $M > M_2$. Comparing with the variation of $< R^2_{g,xy} >$ at $M > M_2$ (Fig. 5), we conclude that the shape is not as sensitive as the size to the surface contact number after the polymer is fully adsorbed. Nevertheless, we find that the asphericity of an adsorbed polymer is always larger than that of a free polymer in bulk solution for all cases we studied. And the change of $\langle A \rangle \approx 0.41$ at $M = 0$ to $\langle A_{xy} \rangle \approx 0.50$ at large M clearly indicates a conformational transition from 3D random coil to 2D random coil.

Finally, snapshots of polymer conformations at several special Ms are presented in Fig. 9 for polymer length $N = 100$ with $E_{pp} = 0.1$ and $E_{ps} = 1$. At $M = 1$ the beginning of the adsorption, polymer conformation is a random coil. At $M = M_1 = 10$, 10 monomers are adsorbed on the surface whereas the conformation is almost the same as that at $M = 1$. But the adsorption lowers the mass center of polymer and thus

increases the size $< R_g^2 >$. At $M = M_2 = 30$, all monomers are quite close to the surface and the conformation becomes compact. At big $M = 60$, the polymer sits roughly parallel to the surface. And a 2D conformation has a large size in average. We also find the shape is not spherical for these four snapshots.

The evolution of polymer conformations before $M = M_2 = 30$ seems to follow the simple zipping mechanism of the fast polymer adsorption[19]. The adsorption starts from one or a few of monomers touching the surface, and the adsorption continues with more and more adsorbed on the surface. The conformations before M_2 are similar to that described by the framework of a stem-flower picture[20,21]. It is interesting to see that the conformation has more than one adsorbed region at M_2. The late adsorption may then follow an accelerated zipping mechanism[20]. The detailed adsorption mechanisms of the polymer adsorption will be investigated in our further studies.

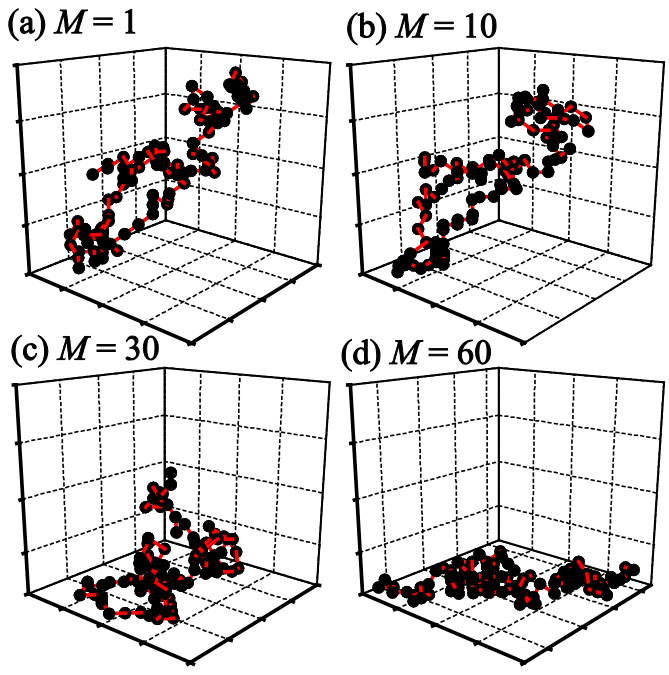

Fig. 9 Snapshots of polymer conformations at the surface contact number M = 1, 10, 30, and 60 for polymer length N = 100 with intra-polymer attraction E_{pp} = 0.1 and polymer-surface attraction E_{ps} = 1. Black solid circles represent monomers of polymer and red lines represent bonds. The four panels have the same surface size (20×20) and height (20). Here, M =10 and 30 are the place of M_1 and M_2, respectively.

We would like to point out that, in order to explain the observation of DNA experiment, our simulation focuses on the adsorption of one single polymer chain. Such a system can well describe the adsorption of polymer at low surface adsorption density where polymer is adsorbed separately on the surface[37]. The adsorption dynamics of polymer chain would however change above a critical density where chain overlap takes place, like the equilibrium properties of polymer[37]. As a same reason, the adsorption dynamics of polymer onto nanoparticles in polymer nanocomposites would be dependent on the size of polymer and that of nanoparticle[38]. On the other hand, a homogeneous surface is adopted in the present simulation. We could expect that the adsorption dynamics of polymer onto heterogeneous and disordered surfaces is more complicated[39]. In fact, the surface in DNA adsorption experiment was covered with randomly distributed adsorption sites[23]. Therefore, the adsorption of polymer onto heterogeneous surfaces reserves further study.

4 Conclusion

The adsorption of a bond fluctuation polymer on an attractive homogeneous solid surface is studied using dynamic Monte Carlo simulation. The simulation system is embedded in the simple cubic lattice. Simulations are carried out at temperature lower than the critical adsorption point for the polymer. We have calculated polymer's square radius of gyration R_g^2 and its surface parallel component $R_{g,xy}^2$, shape asphericity A, and apparent shape asphericity parallel to surface A_{xy} for polymer with different intra-polymer attractions on different surfaces with different polymer-surface attractions. The dependence of conformational properties of polymer on the simulation time as well as on the surface contact monomer number M is investigated.

Simulation results show that the averaged polymer's conformational size $< R_{g,xy}^2 >$ increases exponentially with time during the transient adsorption process, which is consistent with the recent experimental observation[21]. And the relaxation time decreases with the increase in the polymer-surface attraction. The results are

independent of the intra-polymer attraction of polymer. However we find that the behavior of $<A_{xy}>$ is sensitive to intra-polymer interaction and thus different behaviors are observed for different intra-polymer attraction strengths. It may decrease at the beginning of the adsorption and then increases with time at weak intra-polymer attraction, or it may increase gradually with time at strong intra-polymer attraction. Our results show that the fast transient adsorption process is out-of-equilibrium and the competition between relaxation time and adsorption rate of polymer plays important role in the adsorption.

Moreover, our simulation results show that the two-dimensional behaviors of $R_{g,xy}^2$ and A_{xy} are different from that of the three-dimensional conformational size R_g^2 and shape asphericity A during the adsorption process. During the adsorption, the surface contacted monomer number M increases with time, but R_g^2 and A show novel behavior as they first increase with M at small M, then decrease with M at moderate M and finally increase with M again at large M. Whereas $R_{g,xy}^2$ and A_{xy} first decrease with M and then increase with M during the adsorption.

Acknowledgements

This work was supported by the National Natural Science Foundation of China under Grant Nos. 21174132 and 11374255.

References

1 B. O'Shaughnessy and D. Vavylonis, *J. Phys: Condens. Matter*, 2005, 17, R63.

2 P. G. de Gennes, *Macromolecules*, 1980, 13, 1069.

3 S. T. Milner, *Science*, 1991, 251, 905.

4 B. Xue and W. Wang, *J. Chem. Phys.*, 2005, 122, 194912.

5 W. D. Tian and Y. Q. Ma, *Chem. Soc. Rev.*, 2013, 42, 705.

6 J. Liu, Y. Wu, J. Shen, Y. Gao, L. Zhang, and D. Cao, *Phys. Chem. Chem. Phys.*,

2011, 13, 13058.

7 I. Teraoka, Prog. *Polym. Sci.*, 1996, 21, 89.

8 S. Jun and B. Mulder, *Proc. Natl. Acad. Sci. U.S.A.*, 2006, 103, 12388.

9 M. C. Williams, *Proc. Natl. Acad. Sci. U.S.A.*, 2007, 104, 11125.

10 E. Eisenriegler, K. Kremer and K. Binder, *J. Chem.Phys.*, 1982, 77, 6296.

11 A. Milchev and K. Binder, *Macromolecules*, 1996, 29, 343.

12 R. Descas, J. -U. Sommer, and A. Blumen, *J. Chem. Phys.*, 2004, 120, 8831.

13 H. Li, C. J. Qian, and M. B. Luo, *J. Appl. Poly. Sci.*, 2012, 124, 282.

14 J. Krawczyk, A. L. Owczarek, T. Prellberg, and A. Rechnitzer, *Europhys. Lett.*, 2005, 70, 726.

15 M. Bachmann and W. Janke, *Phys. Rev. Lett.*, 2005, 95, 058102.

16 J. Luettmer-Strathmann, F. Rampf, W. Paul, and K. Binder, *J. Chem. Phys.*, 2008, 128, 064903.

17 Y. W. Li, T. Wüst, and D. P. Landau, *Phys. Rev. E*, 2013, 87, 012706.

18 J. S. Shaffer, *J. Chem. Phys.*, 1994, 101, 4205.

19 A. L. Ponomarev, T. D. Sewell, and C. J. Durning, *Macromolecules*, 2000, 33, 2662.

20 R. Descas, J. -U. Sommer, and A. Blumen, *J. Chem. Phys.*, 2006, 124, 094701.

21 S. Bhattacharya, A. Milchev, V. G. Rostiashvili, A. Y. Grosberg, and T. A. Vilgis, *Phys. Rev. E*, 2008, 77, 061603.

22 E. Guzmán, F. Ortega, M. G. Prolongo, V. M. Starov, and F. G. Rubio, *Phys. Chem. Chem. Phys.*, 2011, 13, 16416.

23 C. M. Chang, Y. G. Lau, J. C. Tsai, and W. T. Juan, *EPL*, 2012, 99, 48008.

24 M. B. Luo and J. H. Huang, *J. Chem. Phys.*, 2003, 119, 2439.

25 I. Carmesin and K. Kremer, *Macromolecules*, 1988, 21, 2819.

26 M. B. Luo and W. P. Cao, *Phys. Rev. E*, 2012, 86, 031914.

27 H. Li, C. J. Qian, C. Wang, and M. B. Luo, *Phys. Rev. E*, 2013, 87, 012602.

28 H. Arkin and W. Janke, *Phys. Rev. E*, 2012, 85, 051802.

29 M. Bishop and C. J. Saltiel, *J. Chem. Phys.*, 1988, 88, 3976.

30 M. Bishop and C. J. Saltiel, *J. Chem. Phys.*, 1988, 88, 6594.

31 M. Bishop, J. H. R. Clarke, A. Rey, and J. J. Freire, *J. Chem. Phys.*, 1991, 95, 608.

32 M. Möddel, W. Janke, and M. Bachmann, *Phys. Chem. Chem. Phys.*, 2010, 12, 11548.

33 M. Moddel, W. Janke, and M. Bachmann, *Macromolecules*, 2011, 44, 9013.

34 R. Chang and A. Yethiraj, *Phys. Rev. Lett.*, 2006, 96, 107802.

35 H. Li, C. J. Qian, L. Z. Sun, and M. B. Luo, *Polym. J.*, 2010, 42, 383.

36 M. B. Luo, J. H. Huang, Y. C. Chen, and J. M. Xu, Euro. *Polym. J.*, 2001, 37, 1587.

37 A. Chremos, E. Glynos, V. Koutsos, and P. J. Camp, *Soft Matter*, 2009, 5, 637.

38 C. C. Lin, S. Gam, J. S. Meth, N. Clarke, K. I. Winey, and R. J. Composto, *Macromolecules*, 2013, 46, 4502.

39 G. Raos and T. J. Sluckin, *Macromol. Theory Simul.*, 2013, 22, 225.